Ultrasound Obstet Gynecol 2022; **59**: 651–659
Published online 6 April 2022 in Wiley Online Library (wileyonlinelibrary.com). **DOI:** 10.1002/uog.24781.

Fetal myocardial deformation measured with two-dimensional speckle-tracking echocardiography: longitudinal prospective cohort study of 124 healthy fetuses

N. H. M. VAN OOSTRUM[1,2,3#], C. M. DE VET[1,2,4#], S. B. CLUR[5], D. A. A. VAN DER WOUDE[1,4], E. R. VAN DEN HEUVEL[1,2,6], S. G. OEI[1,2,4] and J. O. E. H. VAN LAAR[1,2,4]

[1]*Eindhoven MedTech Innovation Centre (e/MTIC), Eindhoven, The Netherlands;* [2]*Department of Electrical Engineering, Eindhoven University of Technology, Eindhoven, The Netherlands;* [3]*Department of Gynaecology and Obstetrics, Ghent University, Ghent, Belgium;* [4]*Department of Gynaecology and Obstetrics, Máxima Medical Centre, Veldhoven, The Netherlands;* [5]*Department of Paediatric Cardiology, Emma Children's Hospital, Academic Medical Center, Amsterdam University Medical Centers, Amsterdam, The Netherlands;* [6]*Department of Mathematics & Computer Science, Eindhoven University of Technology, Eindhoven, The Netherlands*

KEYWORDS: deformation values; fetal strain; pregnancy; strain rate; two-dimensional speckle tracking

CONTRIBUTION

What are the novel findings of this work?
In this study, we report reference values for fetal global longitudinal strain (GLS) and GLS rate (GLSR) obtained in uncomplicated pregnancies with non-anomalous fetuses using two-dimensional speckle-tracking echocardiography. Myocardial deformation values of both ventricles increased (i.e. became less negative) with advancing gestation. This study is the first to test GLS and GLSR reference values for eligibility using a leave-one-individual-out approach.

What are the clinical implications of this work?
Reliable reference values with 5% and 95% prediction limits for fetal myocardial deformation parameters were established. These parameters represent fetal cardiac function, which could be compromised in non-cardiac pregnancy complications. Fetal deformation values in complicated pregnancies should be evaluated according to these reference values.

ABSTRACT

Objectives *Two-dimensional speckle-tracking echocardiography (2D-STE) is a promising technique which allows assessment of fetal cardiac function, and can be used in the evaluation of cardiac and non-cardiac diseases in pregnancy. However, reliable fetal reference values for deformation parameters measured using 2D-STE are needed before it can be introduced into clinical practice. This study aimed to obtain reference values for fetal global longitudinal strain (GLS) and GLS rate (GLSR) measured using 2D-STE and compare right and left ventricular values.*

Methods *This was a prospective longitudinal cohort study of uncomplicated pregnancies that underwent echocardiography every 4 weeks from inclusion at 18–21 weeks until delivery to obtain four-chamber loops of the fetal heart. Left and right ventricular GLS and GLSR were measured using 2D-STE at each examination. Using Bayesian mixed-effects models, reference values with lower and upper 5% prediction limits were calculated according to gestational age. Right and left ventricular GLS values according to gestational age were compared using the Wilcoxon signed-rank test.*

Results *A total of 592 left ventricular and 566 right ventricular GLS and GLSR measurements were obtained from 124 women with uncomplicated pregnancy and non-anomalous, appropriately grown fetuses. Reference values were obtained for both fetal ventricles according to gestational week. GLS and GLSR values of both ventricles increased (i.e. became less negative) significantly during pregnancy. Right ventricular GLS values were significantly higher (i.e. less negative) than the respective left ventricular values at every gestational week.*

Conclusions *Reference values were obtained for fetal GLS and GLSR measured using 2D-STE. GLS and*

Correspondence to: Dr C. M. de Vet, Máxima Medical Centre, De Run 4600, 5504 DB Veldhoven, The Netherlands (e-mail: Chantelle.de.Vet@mmc.nl)

#N.H.M.v.O. and C.M.d.V. contributed equally to this study.

Accepted: 16 September 2021

GLSR values increased significantly for both ventricles from the second trimester until delivery. GLS values were significantly higher for the right ventricle compared with the left ventricle. Future studies are needed to assess whether the obtained reference values are helpful in clinical practice in the assessment of pregnancy complications, such as fetal growth restriction or cardiac anomaly. © *2022 The Authors. Ultrasound in Obstetrics & Gynecology published by John Wiley & Sons Ltd on behalf of International Society of Ultrasound in Obstetrics and Gynecology.*

INTRODUCTION

Given the central role of the fetal heart in the adaptive response to changing hemodynamics, the assessment of fetal cardiac function can be of value in the investigation of several non-cardiac diseases, such as fetal growth restriction or maternal diabetes[1–4]. Assessment of fetal cardiac function can also be useful in the diagnosis and follow-up of congenital heart defects, such as aortic coarctation and hypoplastic left-heart syndrome[5–7]. However, the assessment of fetal cardiac function is challenging, given the small size and motion of the fetal heart, the moving fetus and the negative influence of high maternal body mass index. Fetal cardiac function can be expected to change during pregnancy due to physiological growth and development of the heart and changing loading conditions with advancing gestation[8]. Two-dimensional speckle-tracking echocardiography (2D-STE) is a relatively new technique that allows assessment of cardiac function using myocardial deformation imaging. Global longitudinal strain (GLS) i.e. the percentage change in the cardiac wall length, and GLS rate (GLSR) i.e. the velocity of GLS (/s), reflect myocardial deformation and therefore represent cardiac function. 2D-STE has been shown to be feasible and reproducible in the fetus[9–11]. Being relatively angle independent, 2D-STE is easily applicable in the moving fetus, making it a promising tool for the assessment of fetal heart function[8]. Abnormal fetal myocardial deformation values have been reported in pregnancies complicated by various diseases[4,12–16]. However, the diagnostic and prognostic value of fetal GLS and GLSR has remained uncertain. In addition, to evaluate fetal heart function in disease, normal reference values for myocardial deformation parameters measured using 2D-STE still need to be established. The reliability of previously published data has been limited by small cohort size and cross-sectional design of most studies. Furthermore, use of a third-party software system that is compatible with different ultrasound machines is recommended. This makes the currently available reference values unsuitable for the daily clinical assessment of fetal myocardial function[17–19].

In this longitudinal cohort study, we aimed to establish reference values with 5% and 95% prediction limits for GLS and GLSR in both ventricles using 2D-STE in uncomplicated, singleton pregnancies throughout gestation.

METHODS

This was a prospective longitudinal cohort study performed in a tertiary care teaching hospital in The Netherlands between May 2018 and April 2019. The methods have been reported previously in our study protocol[20]. A longitudinal study design with repeated measurements was used to quantify variation with growth and increasing gestational age (GA)[21]. The medical ethics committee of the Máxima Medical Centre, Veldhoven, The Netherlands, approved the study (NL64999.015.18). All participants provided oral and written informed consent. Healthy women with a low-risk, uncomplicated singleton pregnancy and normal second-trimester anomaly scan were eligible. Exclusion criteria were women suffering from a systemic disease, including diabetes and pre-existing hypertensive disease, and an estimated fetal weight below the 10th percentile for GA. GA was based on first-trimester crown–rump length measurement. Women visiting the antenatal ultrasound department for their second-trimester anomaly scan, scheduled between 18 + 0 and 21 + 6 weeks, were invited consecutively to participate. From inclusion until delivery, fetal heart ultrasound scans were performed to obtain 2D four-chamber clips every 4 weeks with a 1-week difference margin. Women who developed gestational diabetes or hypertensive disease and those who delivered a neonate with birth weight < 10th percentile (corrected for gender and GA at birth) or with congenital or genetic abnormality were excluded from the analysis, as these factors may influence myocardial deformation values[4,12,22–24].

To obtain reference values and 90% prediction intervals for healthy fetuses, a study population of at least 100 uneventful pregnancies was needed. The sample size was based on the parametric method, assuming normal distribution of data[25]. As described in our study protocol, it was calculated that 150 healthy women should be included in the initial cohort to obtain 100 uneventful pregnancies. Fifty participants were expected to be excluded due to inadequate ultrasound data, gestational diabetes, fetal growth restriction or hypertensive disease[9,20,26–28].

Experienced cardiac sonographers (N.H.M.v.O., C.M.d.V.) performed ultrasound assessment following a strict protocol[29]. The four-chamber loops of the fetal heart were acquired using an Epiq W7 ultrasound system (Philips Healthcare, Eindhoven, The Netherlands) with a 9-MHz linear transducer. B-mode image depth was reduced and sector width was narrowed to achieve the highest possible frame rate. Three-second DICOM clips were obtained during fetal rest to ensure that at least one complete heart cycle was included in the clip. The offline cardiac software program (2D Cardiac Performance 1.2) developed by TomTec Imaging Systems GmbH (Munich, Germany) was used to analyze the stored clips. For the speckle-tracking analysis, the clip with the highest frame rate and the optimal contrast between the myocardium, atrioventricular valves and the ventricular cavity was selected. The anatomic M-mode feature of the software was used to identify the beginning and end of a cardiac

cycle within one clip. The M-mode appeared after a line was drawn across the left ventricular (LV) wall through the LV and the septum. The opening and closing of the atrioventricular valves were used to identify a heart cycle, together with the corresponding R-wave in the M-mode. The LV and right ventricle (RV) were tracked semiautomatically after marking the ventricular myocardium from the atrioventricular valves to the apex. If needed, this marking could be corrected manually. The software followed automatically the myocardium and its displacement in every frame included in the clip, and calculated the deformation values (Figure 1).

In the small-sized fetal heart, GLS and GLSR have been suggested to be the most reliable parameters to measure[8]. Therefore, our primary aim was to obtain GLS and GLSR reference values with 5% and 95% prediction limits at each gestational week for the LV and the RV. Second, we aimed to analyze the change in GLS, GLSR and fetal heart rate with advancing gestation and to compare LV-GLS and RV-GLS during pregnancy.

GLS was defined as the fractional change in myocardial length during one cardiac heart cycle, expressed as a percentage. In a contracting heart, GLS represents the change from the end-diastolic to the end-systolic myocardial length. Therefore, GLS represents the shortening of the cardiac wall and is presented as a negative value. A mathematically increased (i.e. less negative) GLS value suggests less shortening, while a mathematically decreased (i.e. more negative) value suggests more shortening. GLSR was defined as the velocity of strain (/s).

Statistical analysis was conducted using the statistical software package SPSS, version 22 (IBM Corp., Armonk, NY, USA) and the MIXED procedure of SAS software, version 9.4 (SAS Inc., Cary, NC, USA). The Shapiro–Wilk test was used to determine the normality of distribution of baseline characteristics data. Continuous variables were presented as mean ± SD or median (interquartile range (IQR)), as appropriate. Categorical variables were expressed as *n* (%).

To estimate individual time profiles for the primary variables, LV-GLS, RV-GLS, LV-GLSR and RV-GLSR, from 18 weeks onwards, a linear mixed-effects model for repeated measures was used. Log transformation was used to make the data more normally distributed for LV-GLSR, RV-GLSR and heart rate.

The initial selected time profile was a quadratic function of time with a mean intercept, slope and quadratic term, which were considered multivariate normally distributed and had an unstructured variance-covariance matrix. Each individual had their own time profile. Within-individual variability (i.e. residuals around the individual time profile) was considered normally distributed with a first-order autocorrelation (time in weeks). The model was estimated using maximum likelihood estimation. To investigate the model's goodness of fit, the need for the first-order autocorrelation against residuals being independent was investigated. Additionally, it was investigated whether the quadratic time profile could be reduced to a linear time profile. Both model simplifications were evaluated using the Bayesian information criterion (BIC).

Depending on the best-fit model, the mean time profile and the different sources of variation between and within individuals were estimated using the restricted maximum likelihood estimation. It was then tested whether the average or central time profile for an outcome changed

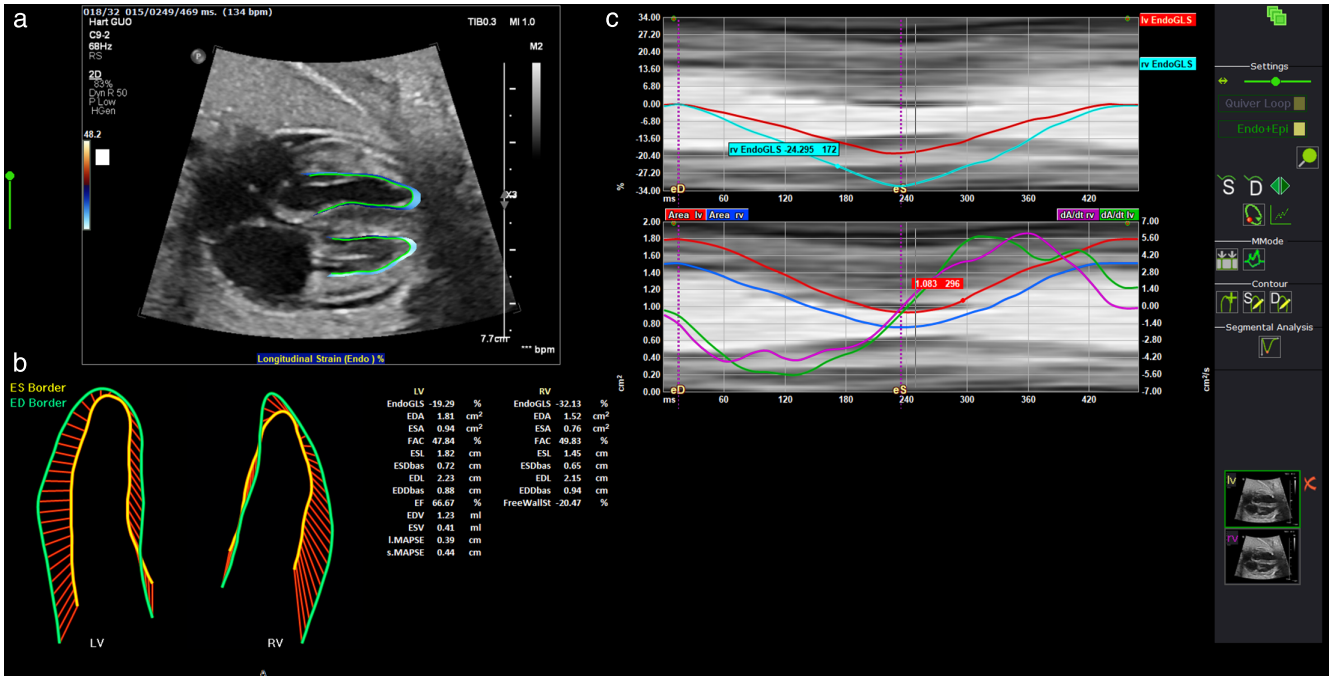

Figure 1 Two-dimensional speckle-tracking analysis, showing marked myocardial region of interest in the left ventricle (LV) and right ventricle (RV) (a), deformation vectors in the LV and RV (b) and LV and RV global longitudinal strain (GLS) analysis (c).

significantly with time or whether the mean outcome was constant. The null hypothesis of a slope being equal to zero was tested for the linear models; for the quadratic models, it was tested whether the quadratic terms were equal to zero. The likelihood ratio test for these null hypotheses was used.

Furthermore, using the model parameters' estimates, lower (5%) and upper (95%) prediction limits (90% prediction intervals) were calculated to represent the reference limits. The calculation was based on the assumption of normality (i.e. the limits were calculated as mean ± 1.64 SD). This mean time profile with these estimated reference limits was visualized together with the individual observations.

To calculate the percentage of observations outside the reference limit, a leave-one-individual-out approach was used. The reference limits were calculated for all individuals except the one individual that was left out. Then, each observation of the left-out individual was compared with the reference limits and coded as one (1) if it fell outside the reference interval or as zero (0) if otherwise. The percentage of observations outside the limits for all individuals who were left out was calculated.

After establishing the LV-GLS and RV-GLS reference values, a Wilcoxon signed-rank test was performed to compare the values between the two ventricles with advancing gestation.

RESULTS

The inclusion of participants in the study is summarized in Figure 2. Initially, 148 women were included. Of these, 24 women were excluded subsequently from further analysis due to the development of hypertension/pre-eclampsia ($n = 4$), gestational diabetes ($n = 9$), birth weight $< 10^{th}$ percentile ($n = 7$), a combination of these three conditions ($n = 3$) or stillbirth ($n = 1$). A total of 124 participants were included finally in the analysis. Their baseline characteristics are presented in Table 1.

A total of 632 DICOM clips were obtained, with a mean number of 5 (range, 2–6) clips per participant. Of these, 40 (6.3%) were excluded from the LV deformation analysis and 66 (10.4%) were excluded from the RV deformation analysis because they were of suboptimal quality. Finally, 592 clips were included in the LV deformation analysis and 566 clips were included in the RV analysis. Overall, a median frame rate of 83 (IQR, 73–96) frames/s was achieved.

Fetal heart rate decreased significantly during pregnancy ($P < 0.001$), from 147 bpm at 18 weeks to 141 bpm at 41 weeks' gestation (Figure 3). The estimated mean values of LV-GLS and RV-GLS and those of LV-GLSR and RV-GLSR together with estimated 5% and 95% prediction limits are provided according to GA in Table 2 and Table 3, respectively. Figure 4 shows GLS and GLSR values and their 5% and 95% prediction limits in both ventricles with increasing GA. The mean regression equations are provided in Figure 4. A tool for automatic calculation of LV-GLS and RV-GLS mean values with prediction limits for a given GA can be found in Appendix S1. Appendix S1 also contains percentiles and *Z*-scores according to GA for any given measurement.

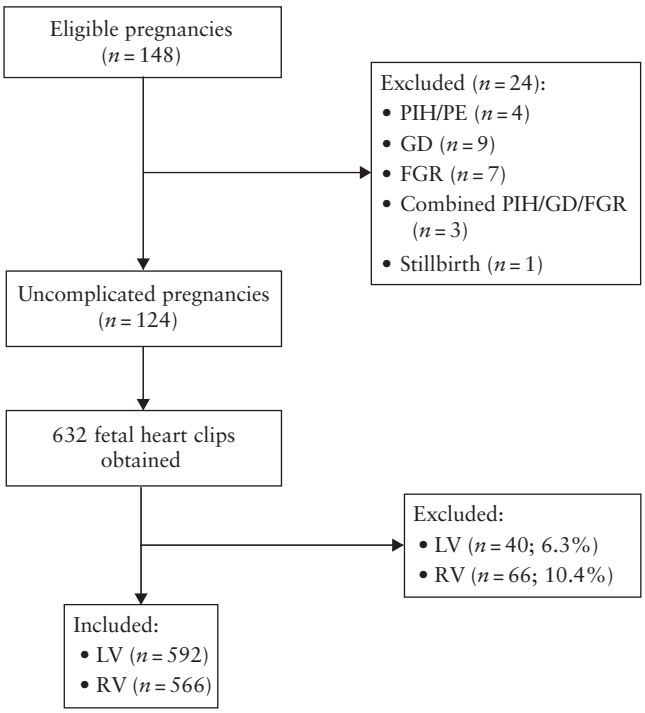

Figure 2 Flowchart summarizing inclusion in the study population of 124 uncomplicated pregnancies with non-anomalous, appropriately grown fetuses and two-dimensional speckle-tracking echocardiographic data collection. FGR, fetal growth restriction; GD, gestational diabetes; LV, left ventricle; PE, pre-eclampsia; PIH, pregnancy-induced hypertension; RV, right ventricle.

Table 1 Baseline characteristics of 124 uncomplicated pregnancies with non-anomalous appropriately grown fetuses included in the study

Characteristic	*Value*
Maternal	
Age (years)	31.9 (29.1–34.1)
BMI (kg/m^2)	22.7 (20.9–26.0)
Nulliparous	68 (54.8)
Smoker	5 (4.0)
Caucasian	108 (87.1)
Mode of delivery	
Vaginal	104 (83.9)
Cesarean	20 (16.1)
Neonatal	
GA at birth (days)	277 (272–285)
Birth weight (g)	3472.5 (3251.2–3720.0)
Birth-weight percentile	50.0 (35.0–76.7)
Female sex	64 (51.6)
5-min Apgar score	9 (9–10)
10-min Apgar score	10 (10–10)
Ultrasound	
Frame rate (frames/s)	83 (73–96)
Frames per cardiac cycle	35 (30–40)

Data are given as median (interquartile range) or *n* (%). BMI, body mass index; GA, gestational age.

The BICs for the two proposed models for each of the five different variables evaluated showed that the linear time profile with independent residuals was the most appropriate model. Investigating the mean time profile for LV-GLS, RV-GLS, LV-GLSR and RV-GLSR showed that all values increased significantly with advancing gestation. All *P*-values were < 0.001. The LV-GLS and RV-GLS values increased by 0.81 and 0.83 percentage points, respectively, per 4 weeks. The LV-GLSR and RV-GLSR values increased by 6.58% and 9.78%, respectively, per 4 weeks. The proportions of observations outside the prediction limits are shown in Table 4. With a maximum of 6% of observations outside the prediction limits, our reference values were shown to be very reliable. From the second trimester onwards, RV-GLS values were significantly higher compared with LV-GLS values (median difference, 2.37 (95% CI, 1.62–3.09); $P < 0.001$).

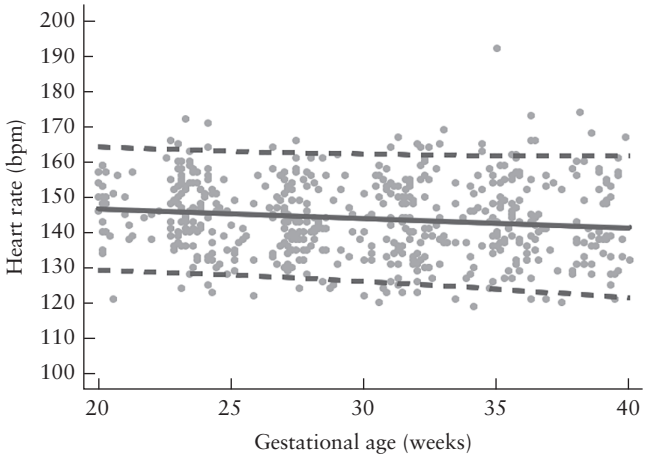

Figure 3 Mean heart rate (—) with 5% and 95% prediction limits (– –) of 124 non-anomalous, appropriately grown fetuses, according to gestational age. Circles are individual datapoints.

DISCUSSION

In this prospective longitudinal cohort study of 124 healthy pregnancies with appropriately grown fetuses, reference values (with 5% and 95% prediction limits) for LV-GLS, LV-GLSR, RV-GLS and RV-GLSR, measured with 2D-STE between 18 and 41 weeks' gestation, were determined. All four parameters were found to increase significantly, suggesting less myocardial shortening with advancing gestation. RV-GLS values were significantly higher than LV-GLS values throughout pregnancy.

Studies aiming to establish reference values require a longitudinal study design with repeated measurements and a population of at least 100 fetuses[25,30]. In contrast to cross-sectional studies, a longitudinal study design allows variation to be quantified over time[21], and avoids bias due to patient-related differences. Seven longitudinal studies on fetal biventricular GLS and GLSR have been conducted to date[27,31–36]. Of these, only two studies included more than 100 fetuses[31,34]. One study reported a significant increase in LV-GLS, LV-GLSR,

Table 2 Estimated mean left (LV) and right (RV) ventricular global longitudinal strain (GLS) with lower (LPL, 5th percentile) and upper (UPL, 95th percentile) prediction limits, according to gestational age (GA)

GA	*LV-GLS (%)*			*RV-GLS (%)*		
(week)	*LPL*	*Mean*	*UPL*	*LPL*	*Mean*	*UPL*
18	−35.82	−23.08	−10.35	−31.43	−20.84	−10.25
19	−35.48	−22.88	−10.27	−31.20	−20.63	−10.06
20	−35.16	−22.68	−10.20	−30.98	−20.42	−9.86
21	−34.84	−22.48	−10.11	−30.77	−20.22	−9.66
22	−34.52	−22.27	−10.02	−30.55	−20.01	−9.47
23	−34.21	−22.07	−9.93	−30.34	−19.80	−9.26
24	−33.91	−21.87	−9.83	−30.12	−19.59	−9.06
25	−33.61	−21.67	−9.72	−29.92	−19.39	−8.85
26	−33.32	−21.46	−9.61	−29.71	−19.18	−8.65
27	−33.03	−21.26	−9.49	−29.51	−18.97	−8.44
28	−32.76	−21.06	−9.36	−29.30	−18.76	−8.22
29	−32.49	−20.86	−9.23	−29.10	−18.56	−8.01
30	−32.22	−20.65	−9.09	−28.91	−18.35	−7.79
31	−31.96	−20.45	−8.94	−28.71	−18.14	−7.57
32	−31.71	−20.25	−8.79	−28.52	−17.93	−7.35
33	−31.47	−20.05	−8.63	−28.33	−17.73	−7.12
34	−31.23	−19.85	−8.46	−28.14	−17.52	−6.90
35	−31.00	−19.64	−8.28	−27.96	−17.31	−6.67
36	−30.78	−19.44	−8.10	−27.77	−17.10	−6.43
37	−30.57	−19.24	−7.91	−27.59	−16.90	−6.20
38	−30.36	−19.04	−7.71	−27.42	−16.69	−5.96
39	−30.16	−18.83	−7.51	−27.24	−16.48	−5.73
40	−29.97	−18.63	−7.29	−27.06	−16.27	−5.48
41	−29.79	−18.43	−7.07	−26.89	−16.07	−5.24

Table 3 Estimated mean left (LV) and right (RV) ventricular global longitudinal strain rate (GLSR) with lower (LPL, 5th percentile) and upper (UPL, 95th percentile) prediction limits, according to gestational age (GA)

GA	*LV-GLSR (/s)*			*RV-GLSR (/s)*		
(week)	*LPL*	*Mean*	*UPL*	*LPL*	*Mean*	*UPL*
18	−3.77	−2.09	−1.16	−3.40	−1.90	−1.06
19	−3.70	−2.06	−1.14	−3.32	−1.86	−1.04
20	−3.63	−2.03	−1.13	−3.25	−1.81	−1.01
21	−3.57	−1.99	−1.11	−3.18	−1.77	−0.99
22	−3.51	−1.96	−1.10	−3.11	−1.73	−0.97
23	−3.45	−1.93	−1.08	−3.04	−1.69	−0.94
24	−3.39	−1.90	−1.07	−2.97	−1.65	−0.92
25	−3.33	−1.87	−1.05	−2.91	−1.62	−0.90
26	−3.28	−1.84	−1.03	−2.85	−1.58	−0.87
27	−3.23	−1.81	−1.02	−2.79	−1.54	−0.85
28	−3.18	−1.78	−1.00	−2.73	−1.51	−0.83
29	−3.13	−1.76	−0.98	−2.68	−1.47	−0.81
30	−3.09	−1.73	−0.97	−2.63	−1.44	−0.79
31	−3.05	−1.70	−0.95	−2.57	−1.41	−0.77
32	−3.01	−1.67	−0.93	−2.52	−1.37	−0.75
33	−2.97	−1.65	−0.91	−2.48	−1.34	−0.73
34	−2.93	−1.62	−0.90	−2.43	−1.31	−0.71
35	−2.89	−1.60	−0.88	−2.38	−1.28	−0.69
36	−2.86	−1.57	−0.86	−2.34	−1.25	−0.67
37	−2.83	−1.55	−0.84	−2.30	−1.22	−0.65
38	−2.80	−1.52	−0.83	−2.26	−1.20	−0.63
39	−2.77	−1.50	−0.81	−2.22	−1.17	−0.62
40	−2.74	−1.47	−0.79	−2.18	−1.14	−0.60
41	−2.71	−1.45	−0.78	−2.14	−1.12	−0.58

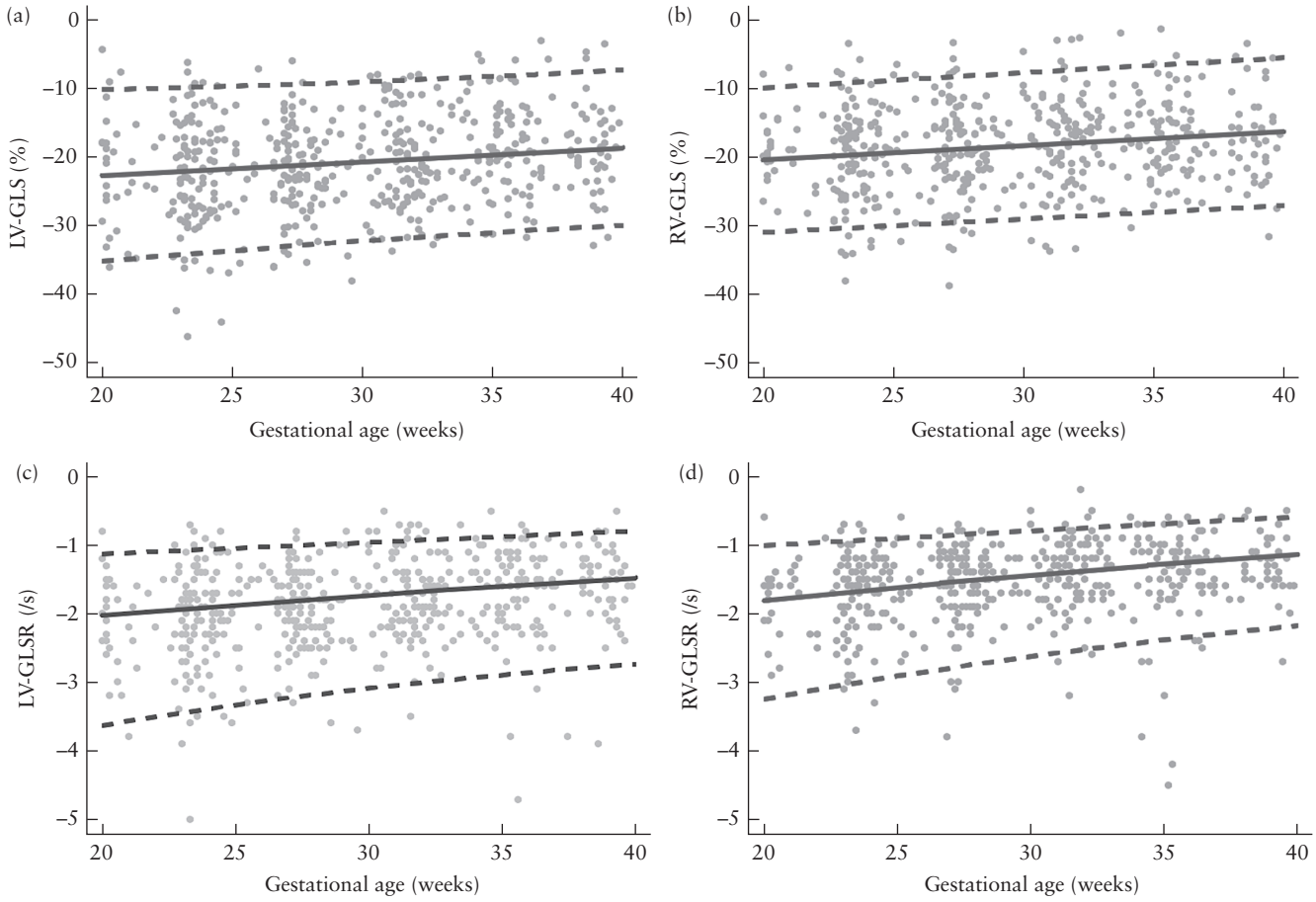

Figure 4 Mean global longitudinal strain (GLS) (a,b) and GLS rate (GLSR) (c,d) (▬) with 5% and 95% prediction limits (▬ ▬) in the left (LV) (a,c) and right (RV) (b,d) ventricle, according to gestational age. The equations of the mean lines are: (a) LV-GLS = −26.73 + 0.2024 weeks and (b) RV-GLS = −24.57 + 0.2074 weeks. Circles are individual datapoints.

Table 4 Percentage of observations for each cardiac parameter outside the lower (LPL) and upper (UPL) prediction limits

Prediction limit	*LV-GLS*	*RV-GLS*	*LV-GLSR*	*RV-GLSR*	*HR*
LPL	5.63	5.11	5.74	5.47	3.67
UPL	4.78	6.00	3.38	4.06	4.47

Data are given as %. GLS, global longitudinal strain; GLSR, GLS rate; HR, heart rate; LV, left ventricle; RV, right ventricle.

RV-GLS and RV-GLSR values at 36, 38 and 40 weeks' gestation[31], which is in agreement with the present study. The second study[34] reported a significant increase in LV-GLS and LV-GLSR values from 18 to 41 weeks but stable RV-GLS and RV-GLSR values with advancing gestation, which was in contrast to our findings. Both studies reported higher strain values compared with our results. To date, 21 studies on fetal GLS and GLSR reference values used a cross-sectional design[11,13,36–54]. Of these, three studies showed an increase in LV-GLS and RV-GLS values throughout gestation[38,44,52], similar to the current study. Other studies reported stable strain values in both ventricles[13,39,40,42,43,48,51,53,54], increased LV-GLS values only[37] or increased RV-GLS values only[36,45,47,49]. The discrepancies among studies can be explained by the differences in ultrasound device and speckle-tracking software used. Speckle-tracking techniques are computer-based, but user dependent for myocardial tracking lines. The moderator band in the RV can cause a suboptimal contrast between the ventricular cavity and endocardium, making tracing more challenging and resulting in inaccuracies in RV deformation values[2,55–57]. Vector velocity imaging (VVI) and 2D-STE software use the same speckle-tracking technique, but different myocardial tracking algorithms. The 2D-STE algorithm tracks the entire myocardial layer to measure deformation values, whereas VVI tracks a narrower myocardial layer[8]. It is thus important that the appropriate reference ranges are available for the software and ultrasound equipment used. This highlights the need for software standardization to make study comparisons possible in the future[58].

Compared with the adult heart, the fetal heart has fewer contractile elements with fewer mitochondria and less organized sarcoplasmic reticula, resulting in a reduced active contraction capacity. Fetal ventricles are stiff and less compliant, and the adrenergic stimulation response is reduced, allowing only limited heart rate adaptation for the maintenance of cardiac output (CO). As the heart develops and grows during gestation, these limitations are reduced, resulting in an increased contraction capacity.

GLS and GLSR of both ventricles can be expected to change during pregnancy, as has been shown in our and other studies[31,38,44], due to the myocardial development combined with changes in preload and afterload[1,59,60]. The equation for CO is stroke volume × heart rate. Stroke volume is dependent positively on preload and contractility and negatively on afterload. GLS is proportional to stroke volume, while GLSR is proportional to CO. Both ventricles provide systemic CO in the fetus due to three essential shunts (ductus venosus, foramen ovale and ductus arteriosus). GLS and GLSR tend to increase (become more negative) with an increase in preload according to the Frank–Starling curve and to reduce (become less negative) with an increase in afterload, and *vice versa*, assuming all other parameters, such as heart rate and contractility, remain equal[59,61,62]. The fetal RV and LV pump 60–65% and 35–40% of the venous return, respectively[1]. Fetal LV preload is determined primarily by umbilical vein flow passing through the foramen ovale under the influence of the size of the opening and the pressure gradient between the atria, as well as by the pulmonary venous return. Thus, with an increase in the pulmonary blood flow in late gestation, LV preload can be expected to increase slightly. LV afterload is determined by the cerebral vascular resistance and the degree of narrowing of the aortic isthmus. The RV is filled predominantly by the systemic venous return from the upper body via the superior vena cava and from the lower body via the inferior vena cava. The majority of its output is via the arterial duct and the descending aorta, as the pulmonary resistance is high due to the uninflated fluid-filled lungs limiting pulmonary blood flow[1]. In late gestation, with increased ductal sensitivity to changes in oxygen, saturation increases and this, along with placental maturation and increasing fetal blood pressure, affects the right ventricular afterload[1,63,64]. Changes in preload and afterload of both ventricles will be reflected in increased GLS and GLSR values. GLSR values will also increase with the reduction in fetal heart rate as GA increases[63]. Furthermore, the whole heart grows and develops, so that, even with a reduction in shortening (less-negative GLS value), the stroke volume increases[65].

In this study, RV-GLS values were shown to be significantly higher throughout pregnancy compared with LV-GLS values. This finding is consistent with the results of other studies comparing LV-GLS and RV-GLS with advancing gestation[34,64,66] and in neonates[67]. Differences in ventricular myocardial architecture can explain the difference in GLS values between the two ventricles[68,69]. The LV myocardium consists of circumferential and longitudinal fibers, leading to deformation in three directions (longitudinal, circumferential and radial)[70]. The RV myofibers are aligned in a more longitudinal direction, resulting in longitudinal shortening.

Strengths and limitations

The strengths of this study are the prospective, longitudinal study design, with more than 100 healthy, appropriately grown fetuses included from 18 weeks' gestation onwards. The established reference values were tested for eligibility using a leave-one-individual-out statistical approach. To our knowledge, we are the first to test for eligibility reference values for fetal myocardial deformation parameters, demonstrating them to be very reliable. Furthermore, the appropriate growth of fetuses was confirmed postnatally. An experienced cardiac sonographer performed ultrasound examinations and the offline 2D-STE analysis. Unfortunately, the derived deformation values could not be compared with those reported in other studies. Speckle-tracking measurements are specific to the ultrasound device and software used, which is a known current limitation of 2D-STE. However, the third-party software used in this study to obtain reference values can be used irrespective of the ultrasound device used. In the future, the use of third-party software could increase the comparability of myocardial deformation values.

Conclusions

In this study, we provide reference values with upper and lower limits for LV-GLS, LV-GLSR, RV-GLS and RV-GLSR, measured with 2D-STE. A gradual increase in all four values from 18 to 41 weeks' gestation was shown. RV-GLS values were higher compared with LV-GLS throughout pregnancy. Future studies are needed to assess whether these reference values are helpful in clinical practice in the identification of pregnancy complications, such as fetal growth restriction or cardiac anomaly. Future research should also focus on vendor-specific differences in reference values. Standardization of software and ultrasound devices used should be achieved before introducing 2D-STE into daily clinical practice.

ACKNOWLEDGMENTS

We thank Philips Healthcare (Eindhoven, The Netherlands) and TomTec Imaging Systems GmbH (Munich, Germany) for providing the software.

REFERENCES

1. Gardiner HM. Response of the fetal heart to changes in load: from hyperplasia to heart failure. *Heart* 2005; **91**: 871–873.
2. Amzulescu MS, De Craene M, Langet H, Pasquet A, Vancraeynest D, Pouleur AC, Vanoverschelde JL, Gerber BL . Myocardial strain imaging: review of general principles, validation, and sources of discrepancies. *Eur Heart J Cardiovasc Imaging* 2019; **20**: 605–619.
3. DeVore GR, Gumina DL, Hobbins JC. Assessment of Ventricular Contractility in Fetuses with an Estimated Fetal Weight Less than the Tenth Centile. *Am J Obstet Gynecol* 2019; **221**: 498.e1–22.
4. Kulkarni A, Li L, Craft M, Nanda M, Lorenzo JMM, Danford D, Kutty S. Fetal myocardial deformation in maternal diabetes mellitus and obesity. *Ultrasound Obstet Gynecol* 2017; **49**: 630–636.
5. Brooks PA, Khoo NS, Mackie AS, Hornberger LK. Right ventricular function in fetal hypoplastic left heart syndrome. *J Am Soc Echocardiogr* 2012; **25**: 1068–1074.
6. Devore GR, Jone PN, Satou G, Sklansky M, Cuneo BF. Aortic Coarctation: A Comprehensive Analysis of Shape, Size, and Contractility of the Fetal Heart. *Fetal Diagn Ther* 2020; **47**: 429–439.
7. Germanakis I, Matsui H, Gardiner HM. Myocardial strain abnormalities in fetal congenital heart disease assessed by speckle tracking echocardiography. *Fetal Diagn Ther* 2012; **32**: 123–130.
8. Germanakis I, Gardiner H. Assessment of fetal myocardial deformation using speckle tracking techniques. *Fetal Diagn Ther* 2012; **32**: 39–46.

9. Di Salvo G, Russo MG, Paladini D, Felicetti M, Castaldi B, Tartaglione A, di Pietto L, Ricci C, Morelli C, Pacileo G, Calabrò R. Two-dimensional strain to assess regional left and right ventricular longitudinal function in 100 normal foetuses. *Eur J Echocardiogr* 2008; **9**: 754–756.
10. Crispi F, Sepulveda-Swatson E, Cruz-Lemini M, Rojas-Benavente J, Garcia-Posada R, Dominguez JM, Sitges M, Bijnens B, Gratacós E. Feasibility and reproducibility of a standard protocol for 2D speckle tracking and tissue Doppler-based strain and strain rate analysis of the fetal heart. *Fetal Diagn Ther* 2012; **32**: 96–108.
11. Ta-Shma A, Perles Z, Gavri S, Golender J, Tarshansky S, Shlichter C, Bar Tov H, Rein AJ. Analysis of segmental and global function of the fetal heart using novel automatic functional imaging. *J Am Soc Echocardiogr* 2008; **21**: 146–150.
12. van Oostrum NHM, van der Woude DAA, Clur SA, Oei SG, van Laar JOEH. Right ventricular dysfunction identified by abnormal strain values precedes evident growth restriction in small for gestational age fetuses. *Prenat Diagn* 2020; **40**: 1525–1531.
13. Van Mieghem T, Giusca S, DeKoninck P, Gucciardo L, Doné E, Hindryckx A, D'Hooge J, Deprest J. Prospective assessment of fetal cardiac function with speckle tracking in healthy fetuses and recipient fetuses of twin-to-twin transfusion syndrome. *J Am Soc Echocardiogr* 2010; **23**: 301–308.
14. Fan X, Zhou Q, Zeng S, Zhou J, Peng Q, Zhang M, Ding Y. Impaired fetal myocardial deformation in intrahepatic cholestasis of pregnancy. *J Ultrasound Med* 2014; **33**: 1171–1177.
15. Miranda JO, Cerqueira RJ, Ramalho C, Areias JC, Henriques-Coelho T. Fetal Cardiac Function in Maternal Diabetes: A Conventional and Speckle-Tracking Echocardiographic Study. *J Am Soc Echocardiogr* 2018; **31**: 333–341.
16. van Oostrum NHM, Derks K, van der Woude DAA, Clur SA, Oei SG, van Laar JOEH. Two-dimensional Speckle tracking echocardiography in Fetal Growth Restriction: a systematic review. *Eur J Obstet Gynecol Reprod Biol* 2020; **254**: 87–94.
17. Amedro P, Bredy C, Guillaumont S, De La Villeon G, Gamon L, Lavastre K, Meli AC, Richard S, Cazorla O, Lacampagne A, Mura T, Vincenti M. Speckle tracking echocardiography in healthy children: comparison between the QLAB by Philips and the EchoPAC by General Electric. *Int J Cardiovasc Imaging* 2019; **35**: 799–809.
18. Manovel A, Dawson D, Smith B, Nihoyannopoulos P. Assessment of left ventricular function by different speckle-tracking software. *Eur J Echocardiogr* 2010; **11**: 417–421.
19. van Oostrum NHM, de Vet CM, van der Woude DAA, Kemps HMC, Oei SG, van Laar JOEH. Fetal strain and strain rate during pregnancy measured with speckle tracking echocardiography: A systematic review. *Eur J Obstet Gynecol Reprod Biol* 2020; **250**: 178–187.
20. van Oostrum NHM, Oei SG, van Laar JOEH. Normal fetal cardiac deformation values in pregnancy; a prospective cohort study protocol. *BMC Pregnancy Childbirth* 2019; **19**: 524.
21. Royston P, Altman DG. Design and analysis of longitudinal studies of fetal size. *Ultrasound Obstet Gynecol* 1995; **6**: 307–312.
22. Aguilera J, Semmler J, Coronel C, Georgiopoulos G, Simpson J, Nicolaides KH, Charakida M. Paired maternal and fetal cardiac functional measurements in women with gestational diabetes mellitus at 35–36 weeks' gestation. *Am J Obstet Gynecol* 2020; **223**: 574.e1–15.
23. Yu L, Zhou Q, Peng Q, Zeng S, Yang Z. Velocity vector imaging echocardiography and NT-proBNP study of fetal cardiac function in pregnancy-induced maternal hypertension. *J Clin Ultrasound* 2019; **47**: 285–291.
24. Semmler J, Garcia-Gonzalez C, Sanchez Sierra A, Gallardo Arozena M, Nicolaides KH, Charakida M. Fetal cardiac function at 35–37 weeks' gestation in pregnancies that subsequently develop pre-eclampsia. *Ultrasound Obstet Gynecol* 2021; **57**: 417–422.
25. Altman DG. *Practical Statistics for Medical Research*. Chapman & Hall/CRC, London, UK; 1990: 422–423.
26. Krause K, Möllers M, Hammer K, Falkenberg MK, Möllmann U, Görlich D, Klockenbusch W, Schmitz R. Quantification of mechanical dyssynchrony in growth restricted fetuses and normal controls using speckle tracking echocardiography (STE). *J Perinat Med* 2017; **45**: 821–827.
27. Li L, Craft M, Hsu HH, Zhang M, Klas B, Danford DA, Kutty S. Left Ventricular Rotational and Twist Mechanics in the Human Fetal Heart. *J Am Soc Echocardiogr* 2017; **30**: 773–780.e1
28. Rolf N, Kerschke L, Braun J, Falkenberg MK, Hammer K, Köster HA, Möllers M, Oelmeier de Murcia K, Klockenbusch W, Schmitz R. Quantification of fetal myocardial function in pregnant women with diabetic diseases and in normal controls using speckle tracking echocardiography (STE). *J Perinat Med* 2018; **47**: 68–76.
29. DeVore GR, Polanco B, Satou G, Sklansky M. Two-Dimensional Speckle Tracking of the Fetal Heart: A Practical Step-by-Step Approach for the Fetal Sonologist. *J Ultrasound Med* 2016; **35**: 1765–1781.
30. Royston P, Wright EM. How to construct 'normal ranges' for fetal variables. *Ultrasound Obstet Gynecol* 1998; **11**: 30–38.
31. Alsolai AA, Bligh LN, Greer RM, Gooi A, Kumar S. Myocardial strain assessment using velocity vector imaging in normally grown fetuses at term. *Ultrasound Obstet Gynecol* 2018; **52**: 352–358.
32. Erickson CT, Levy PT, Craft M, Li L, Danford DA, Kutty S. Maturational patterns in right ventricular strain mechanics from the fetus to the young infant. *Early Hum Dev* 2019; **129**: 23–32.
33. Kapusta L, Mainzer G, Weiner Z, Deutsch L, Khoury A, Haddad S, Lorber A. Changes in fetal left and right ventricular strain mechanics during normal pregnancy. *J Am Soc Echocardiogr* 2013; **26**: 1193–1200.
34. Lee-Tannock A, Hay K, Gooi A, Kumar S. Global longitudinal reference ranges for fetal myocardial deformation in the second half of pregnancy. *J Clin Ultrasound* 2020; **48**: 396–404.
35. Maskatia SA, Pignatelli RH, Ayres NA, Altman CA, Sangi-Haghpeykar H, Lee W. Fetal and Neonatal Diastolic Myocardial Strain Rate: Normal Reference Ranges and Reproducibility in a Prospective, Longitudinal Cohort of Pregnancies. *J Am Soc Echocardiogr* 2016; **29**: 663–669.
36. Ohira A, Hayata K, Mishima S, Tani K, Maki J, Mitsui T, Eto E, Masuyama H. The assessment of the fetal heart function using two-dimensional speckle tracking with a high frame rate. *Early Hum Dev* 2020; **151**: 105160.
37. Biancardi M, De Sa RAM. Behavior of fetal longitudinal myocardial fibers assessed by speckle tracking to obtain strain and strain rate values for low-risk pregnancies. *J Perinat Med* 2020; **48**: 144–152.
38. Clavero Adell M, Ayerza Casas A, Jiménez Montañés L, Palanca Arias D, López Ramón M, Alcalá Nalvaiz J-T, et al. Evolution of strain and strain rate values throughout gestation in healthy fetuses. *Int J Cardiovasc Imaging* 2020; **36**: 59–66.
39. Devore GR, Klas B, Satou G, Sklansky M. Longitudinal annular systolic displacement compared to global strain in normal fetal hearts and those with cardiac abnormalities. *J Ultrasound Med* 2018; **37**: 1159–1171.
40. Enzensberger C, Achterberg F, Degenhardt J, Wolter A, Graupner O, Herrmann J, Axt-Fliedner R. Feasibility and Reproducibility of Two-Dimensional Wall Motion Tracking (WMT) in Fetal Echocardiography. *Ultrasound Int Open* 2017; **3**: E26–33.
41. Enzensberger C, Rostock L, Graupner O, Götte M, Wolter A, Vorisek C, Herrmann J, Axt-Fliedner R. Wall motion tracking in fetal echocardiography-Application of low and high frame rates for strain analysis. *Echocardiography* 2019; **36**: 386–393.
42. Kim SH, Miyakoshi K, Kadohira I, Tanaka M, Minegishi K, Matsumoto T, Yoshimura Y. Comparison of the right and left ventricular performance during the fetal development using velocity vector imaging. *Early Hum Dev* 2013; **89**: 675–681.
43. Liu F, Liu S, Ma Z, Zhan X, Tao G, Cheng L, Song X. Assessment of left ventricular systolic function in fetuses without myocardial hypertrophy of gestational diabetes mellitus mothers using velocity vector imaging. *J Obstet Gynaecol* 2012; **32**: 252–256.
44. Matsui H, Germanakis I, Kulinskaya E, Gardiner HM. Temporal and spatial performance of vector velocity imaging in the human fetal heart. *Ultrasound Obstet Gynecol* 2011; **37**: 150–157.
45. Willruth AM, Geipel AK, Berg CT, Fimmers R, Gembruch UG. Comparison of global and regional right and left ventricular longitudinal peak systolic strain, strain rate and velocity in healthy fetuses using a novel feature tracking technique. *J Perinat Med* 2011; **39**: 549–556.
46. Willruth AM, Geipel A, Berg C, Fimmers R, Gembruch U. Assessment of left ventricular global and regional longitudinal peak systolic strain, strain rate and velocity with feature tracking in healthy fetuses. *Ultraschall der Medizin* 2012; **33**: E293–298.
47. Willruth AM, Geipel AK, Fimmers R, Gembruch UG. Assessment of right ventricular global and regional longitudinal peak systolic strain, strain rate and velocity in healthy fetuses and impact of gestational age using a novel speckle/feature-tracking based algorithm. *Ultrasound Obstet Gynecol* 2011; **37**: 143–149.
48. Younoszai AK, Saudek DE, Emery SP, Thomas JD. Evaluation of Myocardial Mechanics in the Fetus by Velocity Vector Imaging. *J Am Soc Echocardiogr* 2008; **21**: 470–474.
49. Chelliah A, Dham N, Frank LH, Donofrio M, Krishnan A. Myocardial strain can be measured from first trimester fetal echocardiography using velocity vector imaging. *Prenat Diagn* 2016; **36**: 483–488.
50. Miller TA, Puchalski MD, Weng C, Menon SC. Regional and global myocardial deformation of the fetal right ventricle in hypoplastic left heart syndrome. *Prenat Diagn* 2012; **32**: 949–953.
51. Liu M, Yu J, Fu X, Wan W. Quantitative assessment of cardiac function in fetuses of women with maternal gestational thyroid dysfunction using VVI echocardiography. *Med Sci Monit* 2015; **21**: 2956–2968.
52. Truong UT, Sun HY, Tacy TA. Myocardial deformation in the fetal single ventricle. *J Am Soc Echocardiogr* 2013; **26**: 57–63.
53. Dahlbäck C, Gudmundsson S. Increased pulsatility in the fetal ductus venosus is not related to altered cardiac strain in high-risk pregnancies. *J Matern Neonatal Med* 2016; **29**: 1328–1333.
54. Ishii T, McElhinney DB, Harrild DM, Marcus EN, Sahn DJ, Truong U, Tworetzky W. Circumferential and longitudinal ventricular strain in the normal human fetus. *J Am Soc Echocardiogr* 2012; **25**: 105–111.
55. Patey O, Carvalho JS, Thilaganathan B. Intervendor Discordance of Fetal and Neonatal Myocardial Tissue Doppler and Speckle-Tracking Measurements. *J Am Soc Echocardiogr* 2019; **32**: 1339–1349.e23.
56. Koopman LP, Slorach C, Hui W, Manlhiot C, McCrindle BW, Friedberg MK, Jaeggi ET, Mertens L. Comparison between different speckle tracking and color tissue Doppler techniques to measure global and regional myocardial deformation in children. *J Am Soc Echocardiogr* 2010; **23**: 919–928.
57. Day TG, Charakida M, Simpson JM. Using speckle-tracking echocardiography to assess fetal myocardial deformation: are we there yet? *Ultrasound Obstet Gynecol* 2019; **54**: 575–581.
58. Voigt JU, Pedrizzetti G, Lysyansky P, Marwick TH, Houle H, Baumann R, Pedri S, Ito Y, Abe Y, Metz S, Song JH, Hamilton J, Sengupta PP, Kolias TJ, d'Hooge J, Aurigemma GP, Thomas JD, Badano LP. Definitions for a common standard for 2D speckle tracking echocardiography: consensus document of the EACVI/ASE/Industry Task Force to standardize deformation imaging. *J Am Soc Echocardiogr* 2015; **28**: 183–193.
59. Burns AT, La Gerche A, D'hooge J, MacIsaac AI, Prior DL. Left ventricular strain and strain rate: characterization of the effect of load in human subjects. *Eur J Echocardiogr* 2010; **11**: 283–289.
60. Becker M, Kramann R, Dohmen G, Lückhoff A, Autschbach R, Kelm M, Hoffmann R. Impact of left ventricular loading conditions on myocardial deformation parameters: analysis of early and late changes of myocardial deformation parameters after aortic valve replacement. *J Am Soc Echocardiogr* 2007; **20**: 681–689.
61. Fredholm M, Jörgensen K, Houltz E, Ricksten S-E. Load-dependence of myocardial deformation variables - a clinical strain-echocardiographic study. *Acta Anaesthesiol Scand* 2017; **61**: 1155–1165.
62. Ferferieva V, Van den Bergh A, Claus P, Jasaityte R, Veulemans P, Pellens M, La Gerche A, Rademakers F, Herijgers P, D'hooge J. The relative value of strain and

strain rate for defining intrinsic myocardial function. *Am J Physiol Heart Circ Physiol* 2012; **302**: H188–195.
63. Rösner A, Bijnens B, Hansen M, How OJ, Aarsaether E, Müller S, Sutherland GR, Myrmel T. Left ventricular size determines tissue Doppler-derived longitudinal strain and strain rate. *Eur J Echocardiogr* 2009; **10**: 271–277.
64. Alanne L, Bhide A, Lantto J, Huhta H, Kokki M, Haapsamo M, Acharya G, Räsänen J. Nifedipine disturbs fetal cardiac function during hypoxemia in a chronic sheep model at near term gestation. *Am J Obstet Gynecol* 2021; **225**: 544.e1–9.
65. Mielke G, Benda N. Cardiac output and central distribution of blood flow in the human fetus. *Circulation* 2001; **103**: 1662–1668.
66. Willruth AM, Geipel AK, Berg CT, Fimmers R, Gembruch UG. Comparison of global and regional right and left ventricular longitudinal peak systolic strain, strain rate and velocity in healthy fetuses using a novel feature tracking technique. *J Perinat Med* 2011; **39**: 549–556.
67. El-Khuffash A, Schubert U, Levy PT, Nestaas E, de Boode WP. Deformation imaging and rotational mechanics in neonates: a guide to image acquisition, measurement, interpretation, and reference values. *Pediatr Res* 2018; **84** (Suppl 1): 30–45.
68. Petitjean C, Rougon N, Cluzel P. Assessment of myocardial function: a review of quantification methods and results using tagged MRI. *J Cardiovasc Magn Reson* 2005; **7**: 501–516.
69. Buckberg G, Hoffman JIE. Right ventricular architecture responsible for mechanical performance: unifying role of ventricular septum. *J Thorac Cardiovasc Surg* 2014; **148**: 3164–3166.
70. Greenbaum RA, Ho SY, Gibson DG, Becker AE, Anderson RH. Left ventricular fibre architecture in man. *Br Heart J* 1981; **45**: 248–263.

SUPPORTING INFORMATION ON THE INTERNET

The following supporting information may be found in the online version of this article:

Appendix S1 Automatic tool for calculation of mean left ventricular (LV) and right ventricular (RV) global longitudinal strain (GLS) with 5% and 95% prediction limits, according to gestational age